Bioorg. Med. Chem. 46 (2021) 116357

Contents lists available at ScienceDirect

Bioorganic & Medicinal Chemistry

journal homepage: www.elsevier.com/locate/bmc

Development of curcumin-based amyloid β aggregation inhibitors for Alzheimer's disease using the SAR matrix approach

Rohmad Yudi Utomo [a], Yasunobu Asawa [a], Satoshi Okada [a,b], Hyun Seung Ban [c], Atsushi Yoshimori [d], Jürgen Bajorath [e], Hiroyuki Nakamura [a,b,*]

[a] School of Life Science and Technology, Tokyo Institute of Technology, 4259 Nagatsuta-cho, Midori-ku, Yokohama 226-8501, Japan
[b] Laboratory for Chemistry and Life Science, Institute of Innovative Research, Tokyo Institute of Technology, 4259 Nagatsuta-cho, Midori-ku, Yokohama 226-8503, Japan
[c] Korea Research Institute of Bioscience and Biotechnology, Daejeon 34141, South Korea
[d] Institute for Theoretical Medicine, Inc., 26-1, Muraoka-Higashi 2-chome, Fujisawa, Kanagawa 251-0012, Japan
[e] Department of Life Science Informatics, B-IT, LIMES Program Unit Chemical Biology and Medicinal Chemistry, Rheinische Friedrich-Wilhelms-Universität Friedrich-Hirzebruch-Allee 6, 53115 Bonn, Germany

ARTICLE INFO

Keywords:
SAR matrix
Curcumin
Amyloid β
Alzheimer's disease
Neurotoxicity

ABSTRACT

Amyloid β (Aβ) aggregation inhibitor activity cliff involving a curcumin structure was predicted using the SAR Matrix method on the basis of 697 known Aβ inhibitors from ChEMBL (data set 2487). Among the compounds predicted, compound **B** was found to possess approximately 100 times higher inhibitory activity toward Aβ aggregation than curcumin. TEM images indicate that compound **B** induced the shortening of Aβ fibrils and increased the generation of Aβ oligomers in a concentration dependent manner. Furthermore, compound **K**, in which the methyl ester of compound **B** was replaced by the tert-butyl ester, possessed low cytotoxicity on N2A cells and attenuated Aβ-induced cytotoxicity, indicating that compound **K** would have an ability for preventing neurotoxicity caused by Aβ aggregation.

1. Introduction

Since the Global leaders aim to find an effective way of treating Alzheimer's Disease (AD) by 2025[1], many researchers elucidate various therapeutic strategies following recent findings concerning pathophysiological markers. The initial strategy using acetylcholine-based therapy has thus far exerted the most progressive impact with four FDA-approved drugs[2]. However, these compounds only relieve symptoms with moderate clinical efficacy[3]. Other strategies targeting the misfolded Tau protein are challenged by lack of efficacy in clinical trials and drug administration problems[4,5]. Learning from these clinical observations, recent research strategies focus on targeting amyloid β (Aβ) aggregation, following a well-known hypothesis of therapeutic AD intervention[6].

Aβ-targeted strategies, which account for 54% of AD clinical trials, however, encounter several obstacles. A series of trials have been conducted with monoclonal antibodies, such as Solanezumab and Aducanumab, which bind directly to Aβ. Despite its promising efficacies of such antibodies, the immunogenic effect is a critical issue for therapy[7,8]. On the other hand, RS0406, a low-molecular-weight β-sheet breaker, has entered a phase II clinical trial, but no significant clinical improvement has been demonstrated. Therefore, more potent and efficacious Aβ inhibitors are still required[9,10].

Curcumin, a natural polyphenol, was proposed to be a promising candidate with considerable apparent efficacy in transgenic models of AD; however, in phase II clinical trials, non-negligible side effects such as gastrointestinal symptoms were observed[11]. Evaluation of curcumin derivatives has indicated that the two benzene rings, Michael acceptor framework, and length of linkers contribute to the Aβ inhibitory activity[12]. In addition, molecular modeling studies on curcumin in complex with Aβ have suggested contributions of the ketone groups and methoxy substituents on its benzene rings to biological activity[13,14]. So far, over 200 curcumin derivatives have been synthesized to further optimize the curcumin structure as a potential Aβ inhibitor, and some of these compounds have shown a promising apparent inhibition of the Aβ fibril formation[15,16].

* Corresponding author at: Laboratory for Chemistry and Life Science, Institute of Innovative Research, Tokyo Institute of Technology, 4259 Nagatsuta-cho, Midori-ku, Yokohama 226-8503, Japan.
E-mail address: hiro@res.titech.ac.jp (H. Nakamura).

https://doi.org/10.1016/j.bmc.2021.116357
Received 7 July 2021; Received in revised form 30 July 2021; Accepted 1 August 2021
Available online 8 August 2021

We note, however, that curcumins are known as pan assay interference compounds (PAINS)[17] that may give raise to assay artifacts and false-positive activity readouts. Artificial activities of curcumin are intensely debated[18] and special care must be taken to further assess apparent activities of curcuminoids. Nonetheless, in light of previous findings, we have further investigated curcumin derivatives as potential inhibitors of fibril formation. Several lines of evidence are provided in support of true activity of curcumin derivatives we have developed on the basis of curcuminoids available in the ChEMBL database, as reported in the following[19,20]. Specifically, given the uncertainties associated with curcumin activities, we have attempted to systematically explore structural relationships between curcumin derivatives and associated structure–activity relationships. We have reasoned that this analysis scheme would be less vulnerable to anticipated incidents of false-positives reported in the literature than focusing on individual curcumin derivatives.

In this paper, we introduced the success application of SAR Matrix (SARM) to generate novel curcumin derivatives with improved biological activity. We have applied SARM approach[21], which systematically extracts analogue series from compound data sets and organizes series with structurally related cores in individual matrices akin of R-group tables. Through color coding of matrix cells representing compounds, activity information can be included in the analysis. We have recently shown that the SARM method is useful for systematic analysis of SAR data sets. For structurally related analogue series, SARM produces virtual analogues of known active compounds that represent not yet explored combinations of existing core structures and R-groups whose potential activity can be predicted by SARM-based local Free-Wilson models[17]. In general, the activity is gradually changing with compound modifications in the presence of SAR continuity. However, in the presence of SAR discontinuity, the activity can drastically change with small chemical modifications, leading to the formation of an activity cliff (i.e., a pair of structural analogues with a large difference in potency)[22,23]. Local Free-Wilson type QSAR predictions are generally confined to compound subsets forming continuous SARs, but SARMs also enable the detection of activity cliffs in regions of SAR discontinuity.

2. Results and discussion

To construct SARMs for our analysis, 697 known Aβ inhibitors with available IC_{50} value were retrieved from ChEMBL (data set 2487). After the existing curcumin derivatives or analogues were fragmented by systematic cleavage of exocyclic bonds using the SARM methodology, SARMs were obtained including virtual curcumin derivatives, and the activity of several of these derivatives was predicted. (Figure 1). Analyzing the compound distribution across SARMs using the Molecular Grid Map (MGM)[24], we focused on a putative activity cliff associated with virtual analogues **A**–**C** in Figure 1, for which the activity was predicted. An activity cliff is formed by any of these compounds and the known weakly active analogs at adjacent positions in the MGM. All compounds in this activity cliff region possessed distinct benzene substitution patterns with combination of several functional groups such as hydroxyl, methoxy, methyl methoxyacetate, methyl hydroxyacetate, and trifluoromethyl groups. In addition to compounds **A**–**C**, we also synthesized compound **D** as a new curcumin derivative not originating

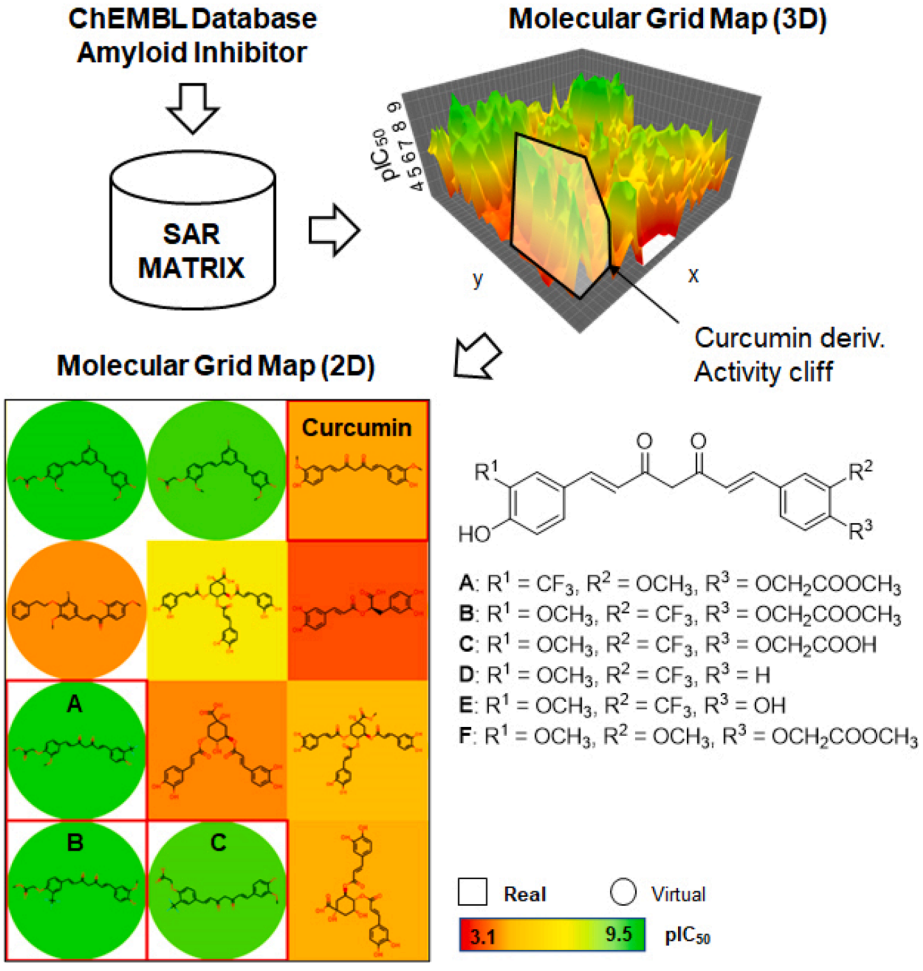

Fig. 1. Activity cliff prediction from SAR Matrix (SARM) method.

from the SARM and compounds **E** and **F** as the reported curcumin derivatives with Aβ-inhibitory activity.

Synthesis of curcumin derivatives **A**–**F** is shown in Scheme 1. Aldehydes **1a**–**b** were chosen as starting materials and reacted with methyl bromoacetate under basic conditions. The resulting aldehyde **2a** underwent the condensation reaction with acetylacetone to give the corresponding conjugated ketone **3a** in 61% yield. The microwave (MW) irradiated condition is essential for this condensation reaction and the desired product **3a** was obtained only in 5% yield without MW irradiation. Further condensation reaction was performed between compound **3a** with compound **1b** to obtain asymmetric curcumin derivative **A**. For obtaining other asymmetric curcumins, first compound **1a** was reacted with acetyl acetone to give compound **4a**. Further condensation reaction with various aldehydes, such as compounds **1b**, **2a-b**, and 3-trifluoromethyl benzaldehyde, produced asymmetric curcumin derivatives **E**, **F**, **B**, and **D**. Compound **C** was obtained from the condensation reaction between compound **2c** (obtained by hydrolysis of compound **2b**) with compound **4a.**

Since the predicted curcumin analogues and their derivatives were successfully synthesized, we next examined the *in vitro* effect of the synthesized compounds on the inhibitory activity of Aβ aggregation. In this study, we choose $Aβ_{42}$ considering as the most neurotoxic Aβ isoform[24]. The aggregation of $Aβ_{42}$ occurred immediately under the biological conditions (pH 7.4), thus could be detected by thioflavin T (ThT) which is known to be interacted on hydrophobic site of $Aβ_{42}$[25]. In this assay, an $Aβ_{42}$ inhibitor was defined by the ability of the compound to competitively interact at the binding site of ThT, resulting in the decreasing of fluorescence intensity during detection. In the case of curcuminoids, results from this assay must be considered with special care[18]. Therefore, detected activities were further investigated, as described below. The results we have obtained using the ThT assay are summarized in Table 1. Curcumin inhibited the aggregation in a dose-dependent manner with the IC_{50} $Aβ_{42}$ value of 0.693 ± 0.013 μM. Further screening using the ThT fluorescence assay revealed that several compounds containing hydroxyl group and methoxycarbonylmethyloxy group on different positions on their benzene ring such as compounds **A**, **B**, and **F** displayed stronger inhibitory activity than curcumin with IC_{50} values of 0.022 ± 0.004, 0.007 ± 0.001, and 0.029 ± 0.005, respectively. In addition, compounds **D** and **E**, which do not contain a methoxycarbonylmethyloxy group but contain a hydroxyl group, also exhibited comparable inhibitory activity to compound **F**, indicating a crucial role for the trifluoromethyl and hydroxyl groups. Although the presence of the carboxymethyloxy group and hydroxyl group on different benzene rings decreased the inhibitory activity, the activity was still comparable to curcumin as shown by compound **C**. We also

Table 1
Inhibition of Aβ aggregation using ThT assay[a]

Compound	IC_{50} (μM) [b]
A	0.022 ± 0.013
B	0.007 ± 0.001
C	0.698 ± 0.010
D	0.013 ± 0.002
E	0.052 ± 0.006
F	0.029 ± 0.005
Curcumin	0.693 ± 0.013
Tacrine	0.022 ± 0.043

[a] The ThT fluorescence assay was carried out by incubating 20 μM of Aβ with serial concentration of curcumin derivatives in PBS pH 7.4 at 37 °C. [b] The drug concentration required to inhibit Aβ aggregation by 50% (IC_{50}) was determined from semi-logarithmic dose–response plots, and results represent the mean ± s.d. of triplicate samples.

confirmed the ability of SARM to predict the Aβ inhibitory activity of novel curcumin derivatives. On the basis of the data we obtained, SARM analysis was continued in search of other promising derivatives.

The results observed from ThT fluorescence assay revealed that several curcumin derivatives possessed higher Aβ aggregation inhibitory activity than curcumin. Therefore, we updated the SARM analysis by including the experimental IC_{50} values of all compounds to find other more potent curcumin derivatives. The revised SARM analysis revealed several other curcumin derivatives, including novel compounds **G**, **H**, **I**, and **J**, possessing more potent inhibitory activity than curcumin and comparable with compound **B** (Figure S1).

Synthetic routes for the preparation of compounds **G**, **H**, **I**, and **J**, which were derived from the updated-SARM analysis are also shown in Scheme 1. The compounds **G** and **H** were prepared by reacting compound **3a** with 3-trifluoromethyl benzaldehyde and compound **2b**, respectively. For compounds **I** and **J** were obtained from condensation reaction between compound **4b** with 3-trifluoromethyl benzaldehyde or compound **2b**. Furthermore, we also synthesized compound **K**, a derivative of compound **B**, in which the methyl ester was replaced by the *tert*-butyl ester. The *tert*-butyl group was first introduced on compound **1b**, and the resulting compound **5** was treated with **4a** to afford compound **K**.

To further assess SARM predictions, compounds **G**, **H**, **I**, and **J** were tested in the ThT assay (Table 2). The dose-dependent ThT assay showed these curcumin derivatives were more potent than curcumin: their IC_{50} values were 0.018–0.109 μM whereas the IC_{50} of curcumin was 0.693 μM. Interestingly compounds **D** and **I** which have a 3-

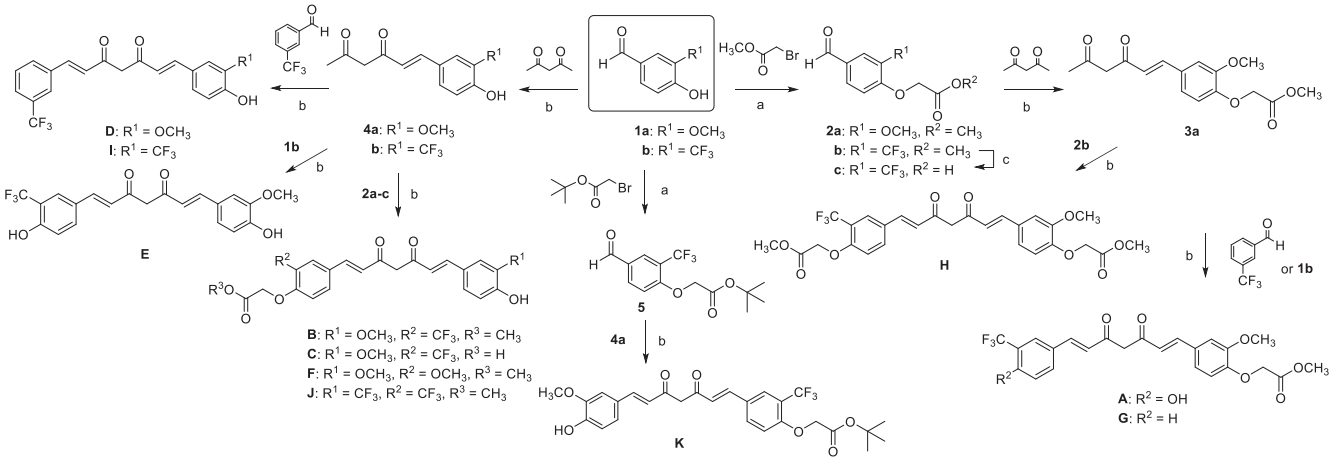

Scheme 1. Synthetic scheme of curcumin derivatives **A**–**K**. Reaction conditions: (a) DMF, K_2CO_3, 80 °C, 2 h; (b) DMF, $B(OH)_3$, morpholine, MW 150 °C, 15 min; (c) NaOH, H_2O, 100 °C, 30 min.

Table 2
Inhibition of Aβ aggregation using ThT assay.

compound	SARM prediction	IC_{50} (μM)
G	8.8	0.046 ± 0.012
H	8.5	0.055 ± 0.009
I	8.8	0.018 ± 0.001
J	8.2	0.109 ± 0.037
K	–	0.055 ± 0.006

trifluoromethylphenyl group in one of two aromatic rings on the curcumin skeleton were more potent than tacrine and comparable with compound **B**. These data indicated the importance of the trifluoromethyl group for the amyloid inhibition activity.

Aggregation of Aβ monomer to oligomers or fibrils has been reported to cause neurotoxicity in Alzheimer's disease[26]. Therefore, we next evaluated whether the synthesized curcumin derivatives prevented the neurotoxicity by inhibiting Aβ aggregation. We chose compounds **B** and **D** as the most potent inhibitors and compound **K** as a derivative of compound **B** for comparison. We used mouse neuroblastoma (N2A) and human glioblastoma (U87MG) cells, that have been commonly used for the Aβ cytotoxicity study of Alzheimer's disease[27,28]. We first examined cell viability of selected curcumin derivatives toward N2A and U87MG cells using 3-(4,5-dimethyl-2-thiazolyl)-2,5-diphenyl-2H-tetrazolium bromide (MTT) assay. The results are summarized in Table 3. Curcumin induced a cytotoxic effect on N2A and U87MG cells with IC_{50} values of 22.6 ± 1.48 and 18.4 ± 3.59, which were similar to those previously reported[29]. In contrast, the curcumin derivatives **B**, **D**, and **K** were less cytotoxic toward both cell lines than curcumin. Especially, compound **K** did not show significant cytotoxicity at 100 μM concentration. We next examined effects of the curcumin derivatives **B** and **K** on Aβ-stimulated cytotoxicity in N2A cells. As expected, Aβ caused a dose-dependent cytotoxic effect on N2A cells as reported[30] (Figure 2A). Next, the effects of compounds **B** and **K** on the viability of N2A cells stimulated by Aβ were evaluated (Figure 2B). The cell viability was reduced to ca. 55% by Aβ (10 μM). In the presence of compound **B** at 1 μM concentration, the cell viability was reduced to ca. 70% with or without Aβ, indicating that compound **B** relieved the Aβ-stimulated cytotoxicity. Indeed, these reduced cell viabilities were caused by the cytotoxicity of compound **B**. Surprisingly, compound **K** was found not only to possess low cytotoxicity but also a significant protective ability against the Aβ-stimulated cytotoxicity, and >90% of cell viability was observed in the Aβ-stimulated cells treated with compound **K**. These results indicated that compound **K** would was able to prevent neurotoxicity caused by Aβ aggregation.

The ThT assay revealed the effectiveness of the curcumin derivatives synthesized in the current study to inhibit Aβ aggregation. To further examine the morphological change after the treatment of Aβ monomer with compound **B**, which would confirm the activity detected in the assays discussed above, we performed negative stained TEM imaging under similar conditions of the ThT assay. As shown in Figure 3, we observed the formation of Aβ fibrils and oligomers, indicated by long-filament surrounded by spherical-shape species[31]. The addition of compound **B** induced shortening of Aβ fibrils and increased the generation of Aβ oligomers in a concentration dependent manner, resulting in the inhibition of the fibril formation from oligomers. These findings provided strong support for the validity of the detected activity of the new curcumin derivatives.

Table 3
Cell viability of selected compounds toward N2A and U87MG cells using MTT assay[a]

compound	IC_{50} (μM)[b]	
	N2A	U87MG
B	38.7 ± 8.47	90.0 ± 5.93
D	65.7 ± 7.44	88.7 ± 2.78
K	>100	>100
Curcumin	22.6 ± 1.48	18.4 ± 3.59

[a] The MTT assay was carried out after treating the cells with serial concentration of curcumin derivatives for 24 h. [b] The drug concentration required to inhibit the cell growth by 50% (IC_{50}) was determined from semilogarithmic dose–response plots, and results represent the mean ± s.d. of three independent experiments in triplicate.

3. Conclusion

In conclusion, we identified compound **B** as a potent Aβ inhibitor from a curcumin-based activity cliff region originating from SARM analysis and revealed by MGM. Compound **B** possessed low cytotoxicity on N2A cells and attenuate Aβ-induced cytotoxicity. Negative stained TEM images indicated that compound **B** induced the shortening of Aβ fibrils and increased the generation of Aβ oligomers in a concentration dependent manner. Furthermore, compound **K** in which the methyl ester of compound **B** was replaced by the *tert*-butyl ester possessed lower cytotoxicity on N2A cells than compound **B** and attenuated Aβ-induced cytotoxicity, indicating that compound **K** has the ability to prevent neurotoxicity caused by Aβ aggregation. Taken together, the results provide several lines of evidence for the relevance of the activities of curcumin derivatives observed in our study, although curcumin has PAINS character and is prone to eliciting assay artifacts.

4. Experimental section

SAR Matrix software beta version was provided under the licensed from Dr. Atsushi Yoshimori from Institute for Theoretical Medicine, Inc, Japan. All the solvents used were in analytical standard grade. The NMR spectra were measured on a Bruker biospin AVANCE II (400 MHz for ^{1}H and 100 MHz for ^{13}C) or a Bruker biospin AVANCE III (500 MHz for ^{1}H, 125 MHz for ^{13}C, and 470 MHz for ^{19}F). Chemical shifts (δ) was reported in ppm relative to internal tetramethylsilane. The HRMS data were recorded on Bruker ESI-TOF-MS micrOTOF II instrument with sodium formate as the calibration standard. Transmission electron microscopy was performed using Hitachi H-8100 operated at 200 kV. Vanillin was purchased from Wako (Japan). Acetylacetone and methyl bromoacetate were purchased from Sigma (USA). Morpholine was purchased from Wako (Japan). The 4-hydroxy-3-(trifluoromethyl) benzaldehyde was purchased from Fluorochem (UK). The 3-(trifluoromethyl) benzaldehyde was purchased from Combi-Blocks (USA). The 4-fluoro-3-(trifluoromethyl) benzaldehyde and *tert*-butyl bromoacetate were purchased from Tokyo Chemical Industry (Japan). Tacrine hydrochloride was purchased from Cayman Chemical (USA). Microwave for synthesis was conducted on Biotage® Initiator + instrument. Column chromatography was performed on silica gel Chromatorex (Japan). Purity analysis of compound A-K was determined by HPLC analysis using Inertsil ODS-3 5 μm (4.6 × 75 mm; GL Science) with a linear gradient of 0.1% formic acid in water/0.1% formic acid in MeCN detected by UV lamp for 25 min. The amyloid β ($Aβ_{42}$) peptide was purchased from Peptide Institute (Japan). The thioflavin T for fluorescence detection of $Aβ_{42}$ was purchased from Sigma (USA). The fluorescence intensity was measured on Tecan Infinite 200.

4.1. Synthesis of compounds

4.1.1. General procedure to Synthesis compound 2a and 2b

Compound 1a or 1b (1 mmol) and potassium carbonate (1 mmol) were dissolved in DMF 10 mL. Methyl bromoacetate (1.1 mmol) was added then the mixture was refluxed for 2 h at 80 °C. The reaction was quenched by HCl 0.1 N then extracted by ethyl acetate. The organic layer was dried using $MgSO_4$ then, purified by column chromatography (silica gel, hexane:ethyl acetate 2:1). **Methyl 2-(4-formyl-2-methoxyphenoxy) acetate (2a).** Yield: 96%. ^{1}H NMR (400 MHz, $CDCl_3$): δ (ppm) 3.86 (–OCH_3, s, 3H), 4.01 (–OCH_3, s, 3H), 4.84 (–CH_2, s, 2H), 6.92

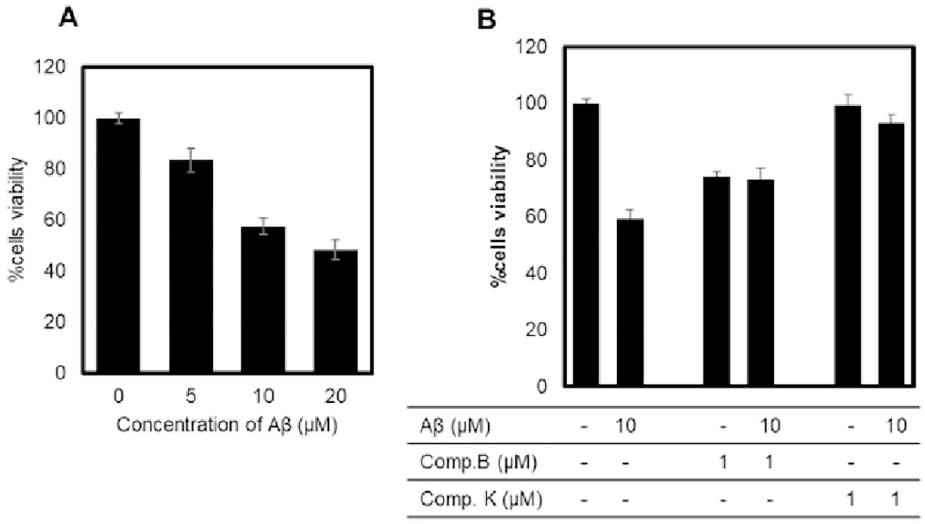

Fig. 2. Curcumin derivatives attenuate Aβ-induced cytotoxicity. (A) Cytotoxic effect of Aβ on N2A cells. (B) Effect of compounds **B** and **K** on the cell viability of Aβ-stimulated N2A cells.

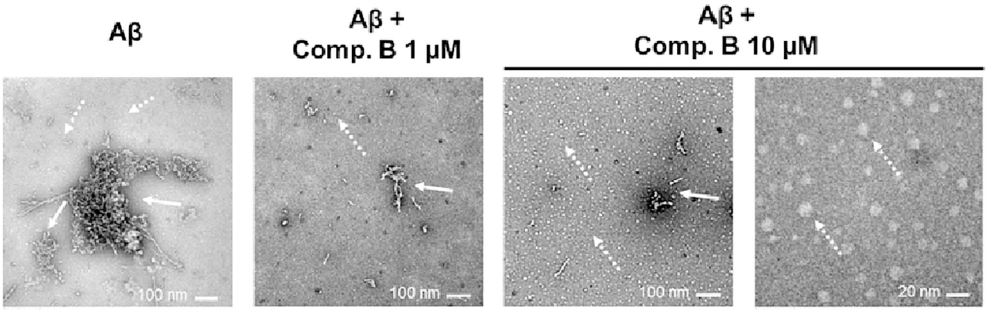

Fig. 3. Negative stained TEM images of Aβ incubated at 37 °C in the absence and presence of Compound B. Fibril (→), oligomer (–>).

(=CH, $J = 8.1$, d, 1H), 7.46 (=CH, $J = 5.5$, 1.8 Hz, dd, 1H), 7.49 (=CH, $J = 1.7$, d, 1H), 9.92 (–CHO, s, 1H). ^{13}C NMR (100 MHz, $CDCl_3$): δ (ppm) 52.89, 56.52, 66.24, 110.34, 112.78, 126.62, 131.59, 150.37, 152.89, 169.01, 190.38. LRMS-ESI (*m/z*): calcd for $C_{11}H_{12}O_5$ 224.07; found 225.09 $[M + H]^+$. **Methyl 2-(4-formyl-2-(trifluoromethyl)phenoxy) acetate (2b).** Yield: 94%. ^{1}H NMR (400 MHz, $CDCl_3$): δ (ppm) 3.82 (–OCH_3, s, 3H), 4.01 (–OCH_3, s, 3H), 4.76 (–CH_2, s, 2H), 6.88 (=CH, $J = 8.8$, d, 1H), 8.05 (=CH, $J = 8.4$, d, 1H), 8.18 (=CH, s, 1H), 9.96 (–OH, s, 1H). ^{13}C NMR (100 MHz, $CDCl_3$): δ (ppm) 52.15, 65.21, 112.86, 119.55 ($J_{C\text{-}F} = 30.7$ Hz, d), 122.69 ($J_{C\text{-}F} = 271.4$ Hz, d), 128.81 ($J_{C\text{-}F} = 5.2$ Hz, d), 129.59, 134.92, 159.97, 159.98, 167.66, 189.54. LRMS-ESI (*m/z*): calcd for $C_{11}H_{19}F_3O_4$ 262.05; found 285.09 $[M + Na]^+$.

4.1.2. General procedure to Synthesis compound 2c

Compound 2b (0.26 mmol) was dissolved in 0.5 mL methanol, then 2 mL of NaOH 1 M was added. The mixture was stirred for 1 h on 100 °C. The reaction was quenched by the addition of HCl 0.1 M then was extracted using ethyl acetate. The desired compound was purified by column chromatography (silica gel, hexane:ethyl acetate 2:1). **2-(4-formyl-2-(trifluoromethyl)phenoxy)acetic acid (2c).** Yield: 41%. ^{1}H NMR (400 MHz, $CDCl_3$): 4.94 (=CH, $J = 8.6$ Hz, d, 1H) 7.08 (=CH, $J = 8.6$ Hz, d, 1H), 8.09 (=CH, $J = 8.7$ Hz, d, 1H), 8.21 (=CH, $J = 1.6$, d, 1H), 9.99 (–CHO, s, 1H). ^{13}C NMR (125 MHz, DMSO-d_6): δ (ppm) 65.43, 68.99, 113.89, 117.19 ($J_{C\text{-}F} = 30.9$ Hz, q), 123.30 ($J_{C\text{-}F} = 270.9$ Hz, q), 123.33, 128.09 ($J_{C\text{-}F} = 5.7$ Hz, q), 128.84 ($J_{C\text{-}F} = 5.6$ Hz, q), 129.31, 135.41, 159.15, 166.04, 169.25, 191.02. LRMS-ESI (*m/z*): calcd for $C_{10}H_7F_3O_4$ 248.03; found 247.12 $[M-H]^-$.

4.1.3. General procedure to Synthesis compound 3a

Compound 3a was synthesized using microwave-assisted reaction. Acetylacetone (20 mmol) and boric acid (20 mmol) were dissolved in DMF. Compound 2a (2 mmol) was added followed by morpholine (0.6 mmol). The mixture was irradiated in microwave at 150 °C for 10 min. The reaction was stopped by the addition of HCl 0.1 N. Crude product was extracted by ethyl acetate then the organic phase was dried using $MgSO_4$. Purification to obtain the desired compound was conducted using column chromatography (silica gel, hexane:ethyl acetate 2:1). **Methyl 2-{4-[(1E)-3,5-dioxohex-1-en-1-yl]-2-methoxyphenoxy}acetate (3a).** Yield: 61%. ^{1}H NMR (400 MHz, $CDCl_3$): δ (ppm) 3.85 (–OCH_3, s, 3H), 3.97 (–OCH_3, s, 3H), 4.78 (–CH_2, s, 2H), 5.69 (–CH_2, s, 2H), 6.39 (=CH, $J = 15.6$ Hz, d, 1H), 6.83 (=CH, $J = 8.8$ Hz, d, 1H), 7.10 (=CH, $J = 6.8$ Hz, d, 1H), 7.12 (=CH, $J = 6.8$ Hz, d, 1H), 7.57 (=CH, $J = 16.0$ Hz, d, 1H).). ^{13}C NMR (125 MHz, CD_3CN): δ (ppm) 27.00, 52.66, 56.42, 66.25, 101.72, 111.66, 114.10, 118.32, 122.18, 122.87, 130.09, 149.94, 150.45, 169.98, 178.59, 198.89. LRMS-ESI (*m/z*): calcd for $C_{16}H_{18}O_6$ 306.11; found 307.02 $[M + H]^+$.

4.1.4. General procedure to Synthesis compound a and G

Compound A and G was synthesized using microwave-assisted reaction. Compound 3a (0.26 mmol) and boric acid (0.26 mmol) was suspended in DMF. Compound Compound 1b or compound 3-trifluoromethyl benzaldehyde (0.26 mmol) was added followed by morpholine (0.1 mmol). The mixture was irradiated in microwave at 150 °C for 10 min. HCl 0.1 N was added to quench the reaction. Crude product was extracted by ethyl acetate then dried using $MgSO_4$. The desired compound was purified by column chromatography (silica gel, hexane:ethyl

acetate 2:1). **Methyl 2-(4-((1E,6E)-7-(4-hydroxy-3-(trifluoromethyl) phenyl)-3,5-dioxohepta-1,6-dien-1-yl)-2-methoxyphenoxy)acetate (A)**. Yield: 40%. ^{1}H NMR (400 MHz, CD_3CN): δ (ppm) 3.76 (–OCH_3, s, 3H), 3.91 (–OCH_3, s, 3H), 4.76 (–CH_2, s, 2H), 5.47 (–CH_2, s, 2H), 5.47 (=CH, s, 1H), 5.97 (=CH, s, 1H), 6.72 (=CH, J = 16.0 Hz, d, 1H), 6.76 (=CH, J = 16.0 Hz, d, 1H), 6.91 (=CH, J = 8.4 Hz, d, 1H), 7.09 (=CH, J = 8.4 Hz, d, 1H), 7.18 (=CH, J = 8.4 Hz, d, 1H), 7.30 (=CH, J = 1.9 Hz, d, 1H), 7.62 (=CH, J = 16.0 Hz, d, 1H), 7.64 (=CH, J = 16.0 Hz, d, 1H), 7.76 (=CH, J = 8.4, 2.0 Hz, dd, 1H), 7.86 (=CH, J = 1.6 Hz, d, 1H), 8.34 (=CH, s, 1H). ^{13}C NMR (125 MHz, DMSO-d_6): δ (ppm) 52.16, 55.99, 58.75, 65.28, 101.67, 111.32, 112.35 ($J_{C\text{-}F}$ = 270.3 Hz, q), 116.36 ($J_{C\text{-}F}$ = 32.1 Hz, q), 117.95, 122.90, 125.95, 127.62, ($J_{C\text{-}F}$ = 4.4 Hz, q), 128.28, 128.50 ($J_{C\text{-}F}$ = 3.8 Hz, q), 128.74, 133.66, 135.82, 139.35, 140.63, 149.37, 157.94, 169.29, 183.31, 183.65. ^{19}F NMR (470 MHz, DMSO-d_6): δ 61.2. HRMS-ESI (m/z): calcd for $C_{24}H_{21}F_3O_7$ 478.1239; found 477.1241 [M−H]$^-$.HPLC purity 94.3%, retention time 5.74 min. **Methyl 2-(4-((1E,6E)-3,5-dioxo-7-(3-(trifluoromethyl)phenyl) hepta-1,6-dien-1-yl)-2-methoxyphenoxy)acetate (G).** Yield: 35%. ^{1}H NMR (400 MHz, $CDCl_3$): δ (ppm) 3.83 (–OCH_3, s, 3H), 3.97 (–OCH_3, s, 3H), 4.77 (–CH_2, s, 2H), 5.85 (–CH_2, s, 1H), 6.55 (=CH, J = 15.8 Hz, d, 1H), 6.69 (=CH, J = 15.8 Hz, d, 1H), 6.83 (=CH, J = 8.7 Hz, d, 1H), 7.13 (=CH, s, 1H), 7.15 (=CH, J = 7.2, 1.8 Hz, dd, 1H), 7.55 (=CH, J = 8.0 Hz, t, 1H), 7.65 (=CH, J = 15.8 Hz, d, 1H), 7.69 (=CH, J = 15.8 Hz, d, 1H), 7.73 (=CH, J = 7.8 Hz, d, 1H), 7.82 (=CH, s, 1H). ^{13}C-NM'R (125 MHz, DMSO-d_6): δ (ppm) 52.01, 55.87, 65.14, 102.08, 111.27, 113.25, 122.71, 122.95, 124.19 ($J_{C\text{-}F}$ = 270.9 Hz, q), 124.82, 126.40, 128.49, 130.02 ($J_{C\text{-}F}$ = 32.8 Hz, q), 130.16, 132.05, 136.11, 138.01, 141.33, 149.27, 149.39, 169.11, 181.21, 185.28. ^{19}F NMR (470 MHz, DMSO-d_6): δ 61.2. HRMS-ESI (m/z): calcd for $C_{24}H_{21}F_3O_6$ 462.1290; found 461.1280 [M−H]$^-$. HPLC purity 90.7%, retention time 6.76 min.

4.1.5. General procedure to Synthesis compound 4a and 4b

Compound 4a and 4b was synthesized using microwave-assisted reaction. Acetylacetone (20 mol) and boric acid (20 mmol) were suspended in DMF. Compound 1a or 1b (2 mmol) was added then followed by morpholine (0.6 mmol). The mixture was irradiated in microwave at 150 °C for 10 min. The reaction mixture was quenched by HCl 0.1 N and extracted using ethyl acetate. The organic phase was dried using $MgSO_4$. The crude product was purified by column chromatography (silica gel, hexane:ethyl acetate 2:1) to obtain the desired compound and curcumin. **(4-hydroxy-3-methoxyphenyl) hex-5-ene-2,4-dione (4a)**. Yield: 65%. ^{1}H NMR (400 MHz, $CDCl_3$): δ (ppm) 2.20 (–CH_3, s, 3H), 3.98 (–OCH_3, s, 3H), 5.68 (=CH, s, 1H), 5.87 (=CH, s, 1H), 6.37 (=CH, J = 15.8, d, 1H), 6.97 (=CH, J = 8.2, d, 1H), 7.06 (=CH, J = 1.8 Hz, d, 1H), 7.13 (=CH, J = 8.2, 1.8 Hz, dd, 1H), 7.58 (=CH, J = 15.8 Hz, d, 1H). ^{13}C NMR (125 MHz, $CDCl_3$): δ (ppm) 26.59, 55.86, 100.69, 111.39, 115.88, 119.87, 123.09, 126.55, 140.47, 148.19, 149.41, 178.48, 196.85. LRMS-ESI (m/z): calcd for $C_{13}H_{14}O_4$ 234.09; found 235.13 [M + H]$^+$. **(E)-6-(4-hydroxy-3-(trifluoromethyl)phenyl)hex-5-ene-2,4-dione (4b).** Yield: 23%. ^{1}H NMR (400 MHz, $CDCl_3$): δ (ppm) 2.20 (–CH_3, s, 3H), 5.67 (–CH_2, s, 1H), 6.41 (=CH, J = 16.0 Hz, d, 1H), 7.01 (=CH, J = 8.4 Hz, d, 1H), 7.57 (=CH, J = 16.0 Hz, d, 1H), 7.61 (=CH, J = 8.4, 1.6 Hz, dd, 1H), 7.70 (=CH, s, 1H). ^{13}C NMR (125 MHz, DMSO-d_6): δ (ppm) 26.79, 101.24, 101.32, 116.53 ($J_{C\text{-}F}$ = 30.1 Hz, q), 117.94, 121.48, 124.15 ($J_{C\text{-}F}$ = 270.9 Hz, q), 125.99, 127.33, 128.24 ($J_{C\text{-}F}$ = 5.2 Hz, q), 133.37, 138.59, 157.93, 177.59, 197.78. LRMS-ESI (m/z): calcd for $C_{13}H_{11}F_3O_3$ 272.07; found 271.03 [M−H]$^+$.

4.1.6. General procedure to Synthesis compound B, C, F, and J

Compound B, C, F, and J was synthesized using microwave-assisted reaction. Compound 4a or 4b (0.26 mmol) and boric acid (0.26 mmol) was suspended in DMF. Compound 2a, 2b, and 2c (0.26 mmol) was added followed by morpholine (0.1 mmol). The mixture was irradiated in microwave at 150 °C for 10 min. The HCl 0.1 N was added to quench the reaction. Crude product was extracted by ethyl acetate then dried using $MgSO_4$. The desired compound was purified by column chromatography (silica gel, hexane:ethyl acetate 2:1). **(1E,6E)-1-(4-hydroxy-3-methoxyphenyl)-7- [3-(trifluoromethyl)phenyl] hepta-1,6-diene-3,5-dione (B)**. Yield: 30%. ^{1}H NMR (400 MHz, DMSO-d_6): 3.72 (–OCH_3, s, 3H), 3.85 (–OCH_3, s, 3H), 5.07 (–CH_2, s, 2H), 6.12 (=CH, s, 1H), 6.81 (=CH, J = 15.8 Hz, d, 1H), 6.83 (=CH, J = 8.1 Hz, d, 1H), 6.93 (=CH, J = 15.9 Hz, d, 1H), 7.18 (=CH, J = 8.1 Hz, d, 1H), 7.2% (=CH, J = 8.8 Hz, d, 1H), 7.34 (=CH, s, 1H), 7.58 (=CH, J = 15.8, d, 1H), 7.63 (=CH, J = 15.9, d, 1H), 7.98 (=CH, J = 8.6, d, 1H), 8.01 (=CH, s, 1H).). ^{13}C NMR (125 MHz, DMSO-d_6): δ (ppm) 52.19, 55.88, 65.29, 101.64, 111.59, 114.36, 115.94, 118.01 ($J_{C\text{-}F}$ = 30.9 Hz, q), 121.29, 123.54, 123.54 ($J_{C\text{-}F}$ = 270.4 Hz, q), 124.19, 126.45, 127.09 ($J_{C\text{-}F}$ = 4.7 Hz, q), 128.17, 133.81, 137.99, 141.68, 148.23, 149.78, 156.70, 168.55, 181.73, 184.89. ^{19}F NMR (470 MHz, DMSO-d_6): δ 60.9. HRMS-ESI (m/z): calcd for $C_{24}H_{21}F_3O_7$ 478.1239; found 477.1235 [M−H]$^-$. HPLC purity 96.1%, retention time 5.88 min. **2-(4-((1E,6E)-7-(4-hydroxy-3-methoxyphenyl)-3,5-dioxohepta-1,6-dien-1-yl)-2-(trifluoromethyl) phenoxy)acetic acid (C).** Yield: 15%. ^{1}H NMR (400 MHz, CD_3CN): 3.98 (–OCH_3, s, 3H), 4.84 (–CH_2, s, 2H), 5.98 (=CH, s, 1H), 6.72 (=CH, J = 16.0 Hz, d, 1H), 6.78 (=CH, J = 16.0 Hz, d, 1H), 6.89 (=CH, J = 8.0 Hz, d, 1H), 7.10 (=CH, J = 8.8 Hz, d, 1H), 7.18 (=CH, J = 8.2, 1.9 Hz, dd, 1H), 7.29 (=CH, J = 1.8 Hz, d, 1H), 7.65 (=CH, J = 15.6 Hz, d, 2H), 7.84 (=CH, J = 8.6 Hz, d, 1H), 7.94 (=CH, J = 1.9 Hz, d, 1H). ^{13}C NMR (125 MHz, DMSO-d_6): δ (ppm) 55.92, 66.81, 101.58, 111.59, 114.52, 115.99, 117.66 ($J_{C\text{-}F}$ = 30.2 Hz, q), 121.29, 122.67, 123.58, 123.74 ($J_{C\text{-}F}$ = 270.7 Hz, q), 126.40, 126.62, 126.74, 127.04 ($J_{C\text{-}F}$ = 4.7 Hz, q), 127.22, 127.49 ($J_{C\text{-}F}$ = 5.2 Hz, q), 133.61, 138.37, 141.62, 141.98, 148.28, 157.84, 170.25, 182.01, 184.68, 198.26. ^{19}F NMR (470 MHz, DMSO-d_6): δ 60.8. HRMS-ESI (m/z): calcd for $C_{23}H_{19}F_3O_7$ 464.1083; found 463.1087 [M−H]$^-$. HPLC purity 96.2%, retention time 5.69 min. **methyl 2-(4-((1E,6E)-7-(4-hydroxy-3-methoxyphenyl)-3,5-dioxohepta-1,6-dien-1-yl)-2-methoxyphenoxy)acetate (F).** Yield: 35%. ^{1}H NMR (400 MHz, $CDCl_3$): δ (ppm) 3.82 (–OCH_3, s, 3H), 3.94 (–OCH_3, s, 3H), 3.94 (–OCH_3, s, 3H), 4.75 (–CH_2, s, 2H), 5.82 (–CH_2, s, 1H), 6.47 (=CH, J = 15.8 Hz, d, 1H), 6.52 (=CH, J = 15.8 Hz, d, 1H), 6.82 (=CH, J = 8.8 Hz, d, 1H), 6.94 (=CH, J = 8.2 Hz, d, 1H), 7.04–7.13 (=CH, m, 4H), 7.58 (=CH, J = 15.8 Hz, d, 1H), 7.62 (=CH, J = 15.8 Hz, d, 1H). ^{13}C NMR (100 MHz, $CDCl_3$): δ (ppm) 52.29, 55.96, 66.15, 101.28, 109.75, 110.87, 113.77, 114.89, 121.76, 122.74, 127.63, 129.65, 139.89, 140.79, 146.86, 147.98, 149.03, 149.75, 169.03, 182.69, 183.78. HRMS-ESI (m/z): calcd for $C_{24}H_{24}O_8$ 440.1471; found 439.1471 [M−H]$^-$. HPLC purity 94.9%, retention time 5.15 min. **methyl 2-(4-((1E,6E)-7-(4-hydroxy-3-(trifluoromethyl)phenyl)-3,5-dioxohepta-1,6-dien-1-yl)-2-(trifluoromethyl)phenoxy)acetate (J).** Yield: 43%. ^{1}H NMR (400 MHz, DMSO-d_6): δ (ppm) 3.72 (–CH_3, s, 3H), 5.07 (–CH_2, s, 2H), 6.14 (–CH_2, s, 1H), 6.89 (=CH, J = 16.0 Hz, d, 1H), 6.98 (=CH, J = 16.0 Hz, d, 1H), 7.10 (=CH, J = 8.4 Hz, d, 1H), 7.27 (=CH, J = 8.8 Hz, d, 1H), 7.62–7.68 (=CH, m, 2H), 7.87 (=CH, J = 8.8 Hz, d, 1H), 7.90 (=CH, s, 1H), 7.99 (=CH, J = 8.7 Hz, d, 1H), 8.02 (=CH, s, 1H). ^{13}C NMR (125 MHz, DMSO-d_6): δ (ppm) 52.20, 65.29, 101.86, 114.41, 116.26 ($J_{C\text{-}F}$ = 30.1 Hz, q), 117.79, 117.96 ($J_{C\text{-}F}$ = 30.5 Hz, q), 122.83, 123.51 ($J_{C\text{-}F}$ = 271.3 Hz, q), 123.92 ($J_{C\text{-}F}$ = 272.5 Hz, q), 124.16, 125.83, 127.18, 127.61 ($J_{C\text{-}F}$ = 4.1 Hz, q), 128.07, 133.70, 133.96, 138.48, 139.65, 156.78, 157.83, 168.55, 182.63, 183.99. ^{19}F NMR (470 MHz, DMSO-d_6): δ 60.9, 61.2. HRMS-ESI (m/z): calcd for $C_{24}H_{18}F_6O_6$ 516.1008; found 515.1008 [M−H]$^-$. HPLC purity 93.4%, retention time 6.33 min.

4.1.7. General procedure to Synthesis compound d and I

Compound D was synthesized using microwave-assisted reaction. Compound 4a (0.26 mmol) and boric acid (0.26 mmol) was suspended in DMF. Compound 3-trifluoromethyl benzaldehyde (0.26 mmol) was added followed by morpholine (0.1 mmol). The mixture was irradiated in microwave at 150 °C for 10 min. The HCl 0.1 N was added to quench the reaction. Crude product was extracted by ethyl acetate then dried using $MgSO_4$. The desired compound was purified by column chromatography (silica gel, hexane:ethyl acetate 2:1). **(1E,6E)-1-(4-hydroxy-3-**

methoxyphenyl)-7-[3-(trifluoromethyl) phenyl] hepta-1,6-diene-3,5-dione (D). Yield: 50%. ^{1}H NMR (400 MHz, $CDCl_3$): 3.98 (–OCH_3, s, 3H), 5.88 (–CH_2, s, 2H), 6.53 (=CH, J = 15.8 Hz, d, 1H), 6.68 (=CH, J = 15.9 Hz, d, 1H), 6.97 (=CH, J = 8.2, d, 1H), 7.09 (=CH, J = 1.5 Hz, d, 1H), 7.17 (=CH, J = 8.2, 1.6 Hz, dd, 1H), 7.55 (=CH, J = 7.8 Hz, t, 1H), 7.65 (=CH, J = 15.8 Hz, d, 1H), 7.68 (=CH, J = 15.9 Hz, d, 1H), 7.73 (=CH, J = 7.8 Hz, d, 1H), 7.82 (=CH, s, 1H). ^{13}C NMR (125 MHz, DMSO-d_6): δ (ppm) 55.89, 102.12, 116.02, 121.38, 123.69, 124.26 ($J_{C\text{-}F}$ = 271.1 Hz, q), 125.78 ($J_{C\text{-}F}$ = 4.1 Hz, q), 126.29, 126.44 ($J_{C\text{-}F}$ = 4.8 Hz, q), 129.58 ($J_{C\text{-}F}$ = 32.1 Hz, q), 129.98, 130.12, 130.27, 131.94, 133.36, 136.25, 137.69, 142.20, 148.31, 150.01, 180.54, 185.96. ^{19}F NMR (470 MHz, DMSO-d_6): δ 61.4. HRMS-ESI (m/z): calcd for $C_{21}H_{17}F_3O_4$ 390.1079; found 389.1069 [M−H]$^-$. HPLC purity 98.8%, retention time 6.78 min. **(1E,6E)-1-(4-hydroxy-3-(trifluoromethyl)phenyl)-7-(3-(trifluoromethyl)phenyl)hepta-1,6-diene-3,5-dione (I)** Yield: 28%. ^{1}H NMR (400 MHz, CD_3CN): δ (ppm) 6.05 (–CH_2, s, 2H), 6.81 (=CH, J = 16.0 Hz, d, 1H), 6.96 (=CH, J = 16.0 Hz, d, 1H), 7.09 (=CH, J = 8.8 Hz, d, 1H), 7.65–7.74 (=CH, m, 3H), 7.78 (=CH, J = 8.4, 2.0 Hz, dd, 1H), 7.88 (=CH, J = 2.1 Hz d, 1H), 7.92 (=CH, J = 7.7 Hz, d, 1H), 7.99 (=CH, s, 1H). ^{13}C NMR (125 MHz, DMSO-d_6): δ (ppm) 48.83, 102.33, 116.39 ($J_{C\text{-}F}$ = 30.1 Hz, q), 117.89, 122.83, 123.99 ($J_{C\text{-}F}$ = 271.3 Hz, q), 124.26 ($J_{C\text{-}F}$ = 270.7 Hz, q), 124.87, 125.72, 126.42, 127.72, 130.14 ($J_{C\text{-}F}$ = 31.6 Hz, q), 130.17, 132.07, 133.72, 136.17, 138.14, 140.16, 158.12, 181.41, 185.11. ^{19}F NMR (470 MHz, DMSO-d_6): δ 61.32, 61.37. HRMS-ESI (m/z): calcd for $C_{21}H_{14}F_6O_3$ 428.0847; found 427.0849 [M−H]$^-$. HPLC purity 93.7%, retention time 7.28 min.

4.1.8. General procedure to Synthesis compound E

Compound E was synthesized using microwave-assisted reaction. Compound 4a (0.26 mmol) and boric acid (0.26 mmol) was suspended in DMF. Compound 1b (0.26 mmol) was added followed by morpholine (0.1 mmol). The mixture was irradiated in microwave at 150 °C for 10 min. The HCl 0.1 N was added to quench the reaction. Crude product was extracted by ethyl acetate then dried using $MgSO_4$. The desired compound was purified by column chromatography (silica gel, hexane: ethyl acetate 2:1). **(1E,6E)-1-(4-hydroxy-3-(trifluoromethyl)phenyl)-7-(4-hydroxy-3-methoxyphenyl)hepta-1,6-diene-3,5-dione (E).** Yield: 28%. Yield: 28%. ^{1}H NMR (400 MHz, CD_3CN): δ (ppm) 3.94 (–OCH_3, s, 3H), 5.96 (–CH_2, s, 1H), 6.70 (=CH, J = 15.6 Hz, d, 1H), 6.74 (=CH, J = 15.6 Hz, d, 1H), 6.89 (=CH, J = 8.0 Hz, d, 1H), 7.08 (=CH, J = 8.4 Hz, d, 1H), 7.17 (=CH, J = 8.4, 1.8 Hz, dd, 1H), 7.28 (=CH, J = 1.8 Hz, d, 1H), 7.61 (=CH, J = 15.6 Hz, d, 2H), 7.75 (=CH, J = 8.6, 1.8 Hz, dd, 1H), 7.86 (=CH, J = 1.6 Hz, d, 1H). ^{13}C NMR (125 MHz, DMSO-d_6): δ (ppm) 55.85, 101.32, 115.86, 116.19 ($J_{C\text{-}F}$ = 30.0 Hz, q), 117.75, 121.22, 121.98 ($J_{C\text{-}F}$ = 271.3 Hz, q), 122.88, 123.46, 124.99, 125.90, 126.42, 127.41 ($J_{C\text{-}F}$ = 4.7 Hz, q), 133.54, 138.84, 141.35, 148.16, 149.63, 157.66, 182.42, 184.22. ^{19}F NMR (470 MHz, DMSO-d_6): δ 61.2. HRMS-ESI (m/z): calcd for $C_{21}H_{17}F_3O_5$ 406.1028; found 405.1022 [M−H]$^-$. HPLC purity 94.1%, retention time 5.63 min.

4.1.9. General procedure to Synthesis compound H

Compound H was synthesized using microwave-assisted reaction. Compound 3a (0.26 mmol) and boric acid (0.26 mmol) was suspended in DMF. Compound 2b (0.26 mmol) was added followed by morpholine (0.1 mmol). The mixture was irradiated in microwave at 150 °C for 10 min. The HCl 0.1 N was added to quench the reaction. Crude product was extracted by ethyl acetate then dried using $MgSO_4$. The desired compound was purified by column chromatography (silica gel, hexane: ethyl acetate 2:1). **Methyl 2-(2-methoxy-4-((1E,6E)-7-(4-(2-methoxy-2-oxoethoxy)-3-(trifluoromethyl)phenyl)-3,5-dioxohepta-1,6-dien-1-yl)phenoxy)acetate (H).** Yield: 38%. ^{1}H NMR (400 MHz, CD_3CN): δ (ppm) 3.77 (–OCH_3, s, 3H), 3.79 (–OCH3, s, 3H), 3.91 (–OCH_3, s, 3H), 4.76 (–CH_2, s, 2H), 4.89 (–CH_2, s, 2H), 6.00 (–CH_2, s, 1H), 6.77 (=CH, J = 15.8 Hz, d, 1H), 6.81 (=CH, J = 15.8 Hz, d, 1H), 6.90 (=CH, J = 8.4 Hz, d, 1H), 7.12 (=CH, J = 8.7 Hz, d, 1H), 7.21 (=CH, J = 8.4, 1.9 Hz, dd, 1H), 7.32 (=CH, J = 1.9 Hz, d, 1H), 7.62 (=CH, J = 15.8 Hz, d, 1H), 7.67 (=CH, J = 15.8 Hz, d, 1H), 7.85 (=CH, J = 8.8, 1.9 Hz, dd, 1H), 7.96 (=CH, J = 1.9 Hz, d, 1H). ^{13}C NMR (125 MHz, DMSO-d_6): δ (ppm) 52.04, 52.20, 55.89, 65.16, 65.28, 101.71, 111.25, 113.28, 143.39, 117.93 ($J_{C\text{-}F}$ = 30.4 Hz, q), 122.42, 122.69, 123.51 ($J_{C\text{-}F}$ = 271.0 Hz, q), 124.19, 127.14 ($J_{C\text{-}F}$ = 4.9 Hz, q), 128.07, 128.59, 133.91, 138.34, 140.86, 149.29, 156.75, 168.54, 169.15, 182.45, 184.22. ^{19}F NMR (470 MHz, DMSO-d_6): δ 60.9. HRMS-ESI (m/z): calcd for $C_{27}H_{25}F_3O_9$ 550.1451; found 549.1449 [M−H]$^-$. HPLC purity 99.8%, retention time 6.52 min.

4.1.10. General procedure to Synthesis compound 5

Compound 1b (1 mmol) and potassium carbonate (1 mmol) were dissolved in DMF 10 mL. *Tert*-butyl bromoacetate (1.1 mmol) was added then was refluxed for 2 h at 80 °C. The reaction was quenched by HCl 0.1 N then extracted by ethyl acetate. The organic layer was dried using $MgSO_4$ then, purified by column chromatography (silica gel, hexane: ethyl acetate 2:1). **Synthesis of (E)-6-(3-(trifluoromethyl)phenyl) hex-5-ene-2,4-dione.** Yield: 97%. ^{1}H NMR (400 MHz, $CDCl_3$): δ (ppm) 1.48 (3x-CH_3, s, 9H), 4.75 (–CH_2, s, 2H), 7.02 (=CH, J = 8.6 Hz, d, 1H), 8.05 (=CH, J = 8.6, 2.0 Hz, dd, 1H), 8.16 (=CH, J = 1.8 Hz, d, 1H), 9.95 (–CHO, s, 1H). ^{13}C NMR (125 MHz, $CDCl_3$): δ (ppm) 27.46, 65.62, 82.69, 112.74, 119.34 ($J_{C\text{-}F}$ = 31.6 Hz, q), 122.71 ($J_{C\text{-}F}$ = 271.1 Hz, q), 128.61 ($J_{C\text{-}F}$ = 5.0 Hz, q), 134.79, 160.10, 166. 06, 189.36. LRMS-ESI (m/z): calcd for $C_{14}H_{15}F_3O_4$ 304.09; found 303.75 [M−H]$^+$.

4.1.11. General procedure to Synthesis compound K

Compound K was synthesized using microwave-assisted reaction. Compound 4a (0.26 mmol) and boric acid (0.26 mmol) was suspended in DMF. Compound 5 (0.26 mmol) was added followed by morpholine (0.1 mmol). The mixture was irradiated by microwave at 150 °C for 10 min. The HCl 0.1 N was added to quench the reaction. Crude product was extracted by ethyl acetate then dried using $MgSO_4$. The desired compound was purified by column chromatography (silica gel, hexane: ethyl acetate 2:1. ***tert*-butyl 2-(4-((1E,6E)-7-(4-hydroxy-3-methoxyphenyl)-3,5-dioxohepta-1,6-dien-1-yl)-2-(trifluoromethyl)phenoxy)acetate (K).** Yield: 28%. ^{1}H NMR (400 MHz, $CDCl_3$): δ (ppm) 1.51 (–CH_3, s, 9H), 3.99 (–CH_3, s, 3H), 4.70 (–CH_2, s, 2H), 5.86 (–CH_2, S, 2H), 6.53 (=CH, J = 16.0 Hz, d, 1H), 6.57 (=CH, J = 16.0 Hz, d, 1H) 6.92 (=CH, J = 8.6 Hz, d, 1H), 6.99 (=CH, J = 8.0 Hz, d, 1H), 7.11 (=CH, s, 1H), 7.19 (=CH, J = 7.9 Hz, d, 1H), 7.61–7.69 (=CH, m, 3H), 7.85 (=CH, s, 1H). ^{13}C NMR (125 MHz, DMSO-d_6): δ (ppm) 27.82, 55.87, 65.61, 81.98, 101.58, 111.56, 114.18, 115.82, 117.89 ($J_{C\text{-}F}$ = 30.5 Hz, q), 121.26, 123.53 ($J_{C\text{-}F}$ = 271.3 Hz, q), 123.56, 124.09, 126.39, 127.11 ($J_{C\text{-}F}$ = 5.5 Hz, q), 127.96, 133.74, 141.66, 148.18, 149.71, 167.06, 181.77, 184.84. ^{19}F NMR (470 MHz, DMSO-d_6): δ 60.9. HRMS-ESI (m/z): calcd for $C_{27}H_{27}F_3O_7$ 520.1709; found 519.1713 [M−H]$^-$. HPLC purity 98.4%, retention time 6.79 min.

4.2. ThT fluorescence assay

Procedure on solubilizing the Aβ was conducted according the known literature by slightly modification[32]. To prepare the Aβ monomer stock, in amount 0.5 mg of the lyophilized Aβ (Peptide Institute) was dissolved in NaOH 2 mM by gently mixing without vortexing to obtain 500 μM as final concentration. The solution was centrifuged at 13,200 rpm, 4 °C, and 10 min. The supernatant was collected and stored in −80 °C. The ability of curcumin derivatives to inhibit $A\beta_{42}$ Aggregation was determined using a thioflavin T (ThT)-based fluorescence assay. This assay was conducted in 96-well plate full black non-binding with frequent 15 s of linear shaking every 5 min and constant heating at 37 °C for three hours. The Thioflavin T (ThT) stock at concentration 200 μM was freshly prepared in tris glycine 10 mM pH 8.5. For assay system, the ThT was diluted by PBS 7.4 to reach concentration 20 μM in each well. Curcumin stock 10 mM was diluted in each well to obtain 10-fold dilution (1, 0.1, 0.01, 0.001, 0.0001, and 0.00001 μM). The Aβ stock was transferred to each well to reach final concentration 20 μM. The

fluorescence intensity was immediately measured with an excitation of 430 nm and emission 480 nm using microplate reader (Tecan Infinite F200, Tecan, Switzerland). The data of fluorescence intensity was corrected toward blank containing PBS and ThT while the IC_{50} values obtained by plotting the intensity at half V_{max} of each group toward concentration.

4.3. MTT assay

The N2A and U87 MG cells were suspended in Dulbecco's Modified Eagle Medium (DMEM) medium supplemented with 10% fetal bovine serum. Briefly, N2A cells ($8x10^3$ cells/well) and U87 MG ($8x10^3$ cells/well) was grown on 96-well plate overnight at 37 °C CO_2 5%. For the single treatment on N2A and U87MG using curcumin derivatives, cells were treated by serial concentration of curcumin, compound B, D, and K (1, 5, 10, 25, 50, 100, and 200 μM). To screen the toxicity of Aβ, N2A cells were treated by Aβ at concentration of 5, 10 and 20 μM. Evaluation of protective effect was conducted by treating the N2A cells with Aβ 10 μM with or without curcumin derivatives 1 μM. An MTT reduction assay was conducted as described previously[33]. Briefly, MTT powder was dissolved in PBS pH 7.4 to obtain 5 mg/mL concentration stock, then was diluted into 0.5 mg/mL in DMEM medium. After removal of medium on 96-well plate containing-treated cell, each well was added by 100 μL MTT 0.5 mg/mL and incubated at 37 °C CO_2 5%. After 3 h incubation, 100 μL DMSO was added following the absorbance measurement at wavelength of 550 nm using microplate reader (Tecan Infinite F200, Tecan, Switzerland). Calculation of % cells viability was measured by dividing the absorbance of untreated cells with the absorbance of curcumin-treated cells.

4.4. Negative-Staining TEM imaging

The negative-staining TEM images were obtained according to the following procedure. Elastic carbon grids (ELS-C10, STEM, Japan) was made hydrophilic using an ion coater (IB-2, Eiko, Japan) with 3 mA of plasma current for 40 s before applying sample solution. 5 μM of Aβ only or in combination with compound B was incubated on PBS pH 7.4 at 37 °C for 30 min. Briefly, 5 μL of the Aβ sample was applied to a hydrophilic grid and incubated for one minute at RT. After gently dried with filter paper, the grid sample was washed with Milli-Q water and dried again with filter paper three times. Finally, the grid was incubated with 5 μL of 1% Nano-W negative staining solution (NY, USA) for one minute followed by complete drying using filter paper. The negative stained sample was observed using TEM H-8100 (Hitachi) operated at 200 kV.

Declaration of Competing Interest

The authors declare that they have no known competing financial interests or personal relationships that could have appeared to influence the work reported in this paper.

Acknowledgments

We thank Prof. Kenjiro Ono (Showa University Medical School), Prof. Mayumi Tsuji (Showa University Pharmacological Research Center), and Prof. Motomu Kanai (Graduate School of Pharmaceutical Sciences, The University of Tokyo) for their valuable suggestions and Prof. Yoshitaka Kitamoto (Tokyo Institute of Technology) for the technical support with TEM measurements. H. S. Ban thanks Five-star Alliance overseas researcher invitation program in "NJRC Mater. & Dev.".

Appendix A. Supplementary data

Supplementary data to this article can be found online at https://doi.org/10.1016/j.bmc.2021.116357.

References

1 Vradenburg G. A pivotal moment in Alzheimer's disease and dementia: how global unity of purpose and action can beat the disease by 2025. *Expert Rev Neurother.* 2015;15(1):73–82.
2 Cummings J, Aisen PS, DuBois B, et al. Drug development in Alzheimer's disease: the path to 2025. *Alz Res Therapy.* 2016;8(1). https://doi.org/10.1186/s13195-016-0207-9.
3 Schneider LS, Sano M. Current Alzheimer's disease clinical trials: Methods and placebo outcomes. *Alzheimers Dement.* 2009;5(5):388–397.
4 Gauthier S, Feldman HH, Schneider LS, et al. Efficacy and safety of tau-aggregation inhibitor therapy in patients with mild or moderate Alzheimer's disease: a randomised, controlled, double-blind, parallel-arm, phase 3 trial. *Lancet.* 2016;388(10062):2873–2884.
5 Lee HE, Lim D, Lee JY, Lim SM, Pae AN. Recent tau-targeted clinical strategies for the treatment of Alzheimer's disease. *Future Med Chem.* 2019;11(15):1845–1848.
6 Scheltens P, Blennow K, Breteler MMB, et al. Alzheimer's disease. *Lancet.* 2016;388(10043):505–517.
7 Honig LS, Vellas B, Woodward M, et al. Trial of Solanezumab for Mild Dementia Due to Alzheimer's Disease. *N Engl J Med.* 2018;378(4):321–330.
8 Schneider L. A resurrection of aducanumab for Alzheimer's disease. *Lancet Neurol.* 2020;19(2):111–112.
9 O'Hare E, Scopes DIC, Kim E-M, et al. Orally bioavailable small molecule drug protects memory in Alzheimer's disease models. *Neurobiol Aging.* 2013;34(4):1116–1125.
10 Nakagami Y, Nishimura S, Murasugi T, et al. A novel β-sheet breaker, RS-0406, reverses amyloid β-induced cytotoxicity and impairment of long-term potentiation in vitro. Br J Pharmacol. 2002;137(5):676-682.
11 Ringman JM, Frautschy SA, Teng E, et al. Oral curcumin for Alzheimer's disease: tolerability and efficacy in a 24-week randomized, double blind, placebo-controlled study. *Alz Res Therapy.* 2012;4(5):43. https://doi.org/10.1186/alzrt146.
12 Reinke AA, Gestwicki JE. Structure–activity Relationships of Amyloid Beta-aggregation Inhibitors Based on Curcumin: Influence of Linker Length and Flexibility. *Chem Biol Drug Des.* 2007;70(3):206–215.
13 Ono K, Hasegawa K, Naiki H, Yamada M. Curcumin has potent anti-amyloidogenic effects for Alzheimer's β-amyloid fibrils in vitro. *J Neurosci Res.* 2004;75(6):742–750.
14 Rao PPN, Mohamed T, Teckwani K, Tin G. Curcumin Binding to Beta Amyloid: A Computational Study. *Chem Biol Drug Des.* 2015;86(4):813–820.
15 Bairwa K, Grover J, Kania M, Jachak SM. Recent developments in chemistry and biology of curcumin analogues. *RSC Adv.* 2014;4(27):13946. https://doi.org/10.1039/c4ra00227j.
16 Chen M, Du Z-Y, Zheng Xi, Li D-L, Zhou R-P, Zhang K. Use of curcumin in diagnosis, prevention, and treatment of Alzheimer's disease. *Neural Regen Res.* 2018;13(4):742. https://doi.org/10.4103/1673-5374.230303.
17 Baell JB, Holloway GA. New Substructure Filters for Removal of Pan Assay Interference Compounds (PAINS) from Screening Libraries and for Their Exclusion in Bioassays. *J Med Chem.* 2010;53(7):2719–2740.
18 Nelson KM, Dahlin JL, Bisson J, Graham J, Pauli GF, Walters MA. The Essential Medicinal Chemistry of Curcumin. *J Med Chem.* 2017;60(5):1620–1637.
19 Chainoglou E, Hadjipavlou-Litina D. Curcumin in Health and Diseases: Alzheimer's Disease and Curcumin Analogues, Derivatives, and Hybrids. *Int J Mol Sci.* 2020;21(6):1975.
20 Shabbir U, Rubab M, Tyagi A, Oh D-H. Curcumin and Its Derivatives as Theranostic Agents in Alzheimer's Disease: The Implication of Nanotechnology. *Int J Mol Sci.* 2021;22(1):196.
21 Asawa Y, Yoshimori A, Bajorath J, Nakamura H. Prediction of an MMP-1 inhibitor activity cliff using the SAR matrix approach and its experimental validation. *Sci Rep.* 2020;10(1):14710.
22 Wassermann AM, Haebel P, Weskamp N, Bajorath J. SAR Matrices: Automated Extraction of Information-Rich SAR Tables from Large Compound Data Sets. *J Chem Inf Model.* 2012;52(7):1769–1776.
23 Gupta-Ostermann D, Shanmugasundaram V, Bajorath J. Neighborhood-Based Prediction of Novel Active Compounds from SAR Matrices. *J Chem Inf Model.* 2014;54(3):801–809.
24 Pike CJ, Burdick D, Walencewicz AJ, Glabe CG, Cotman CW. Neurodegeneration induced by beta-amyloid peptides in vitro: the role of peptide assembly state. *J Neurosci.* 1993;13(4):1676–1687.
25 Sulatskaya AI, Sulatsky MI, Antifeeva IA, Kuznetsova IM, Turoverov KK. Structural Analogue of Thioflavin T, DMASEBT, as a Tool for Amyloid Fibrils Study. *Anal Chem.* 2019;91(4):3131–3140.
26 Um JW, Nygaard HB, Heiss JK, et al. Alzheimer amyloid-β oligomer bound to postsynaptic prion protein activates Fyn to impair neurons. *Nat Neurosci.* 2012;15(9):1227–1235.
27 Bettayeb K, Oumata N, Zhang Y, et al. Small-molecule inducers of Aβ-42 peptide production share a common mechanism of action. *FASEB J.* 2012;26(12):5115–5123.
28 Li Y, Cheng D, Cheng R, et al. Mechanisms of U87 Astrocytoma Cell Uptake and Trafficking of Monomeric versus Protofibril Alzheimer's Disease Amyloid-β Proteins. Ferreira ST, ed. PLoS ONE. 2014;9(6):e99939.
29 Sidhar H, Giri RK. Induction of Bex genes by curcumin is associated with apoptosis and activation of p53 in N2a neuroblastoma cells. *Sci Rep.* 2017;7(1):41420.
30 Yang T, Zhu Z, Yin E, et al. Alleviation of symptoms of Alzheimer's disease by diminishing Aβ neurotoxicity and neuroinflammation. *Chem Sci.* 2019;10(43):10149–10158.

31 Xiao Y, Matsuda I, Inoue M, Sasahara T, Hoshi M, Ishii Y. NMR-based site-resolved profiling of β-amyloid misfolding reveals structural transitions from pathologically relevant spherical oligomer to fibril. *J Biol Chem.* 2020;295(2):458–467.

32 Mohamed T, Shakeri A, Tin G, Rao PPN. Structure-Activity Relationship Studies of Isomeric 2,4-Diaminoquinazolines on β-Amyloid Aggregation Kinetics. *ACS Med Chem Lett.* 2016;7(5):502–507.

33 Mosmann T. Rapid colorimetric assay for cellular growth and survival: Application to proliferation and cytotoxicity assays. *J Immunol Methods.* 1983;65(1-2):55–63.